Research on determining the position of zero optical path difference with the wavelet transform*

QIN Yusheng[1,2], HAN Xin[1], LI Xiangxian[1], TONG Jingjing[1], LI Yan[1], and GAO Minguang[1]**

1. Anhui Institute of Optics and Fine Mechanics, Hefei Institutes of Physical Science, Chinese Academy of Sciences, Hefei 230031, China

2. University of Science and Technology of China, Hefei 230026, China

(Received 1 September 2022; Revised 31 October 2022)

Due to the error of digital sampling, there is a deviation between the zero optical path difference (ZOPD) detection position of the interference signal in the infrared gas analyzer and the actual position. To solve this problem, a high-precision detection method of the ZOPD position based on wavelet transform is proposed. Firstly, the wavelet envelope curve of the interference signal is obtained by the wavelet transform, which can obtain the phase information and amplitude information of the maximum modulation position, and then the optimal ZOPD position is calculated by using the amplitude and phase information. The experimental results show that the error of the wavelet transform method is 19.617 nm, and the relative error is reduced by 93.11% compared with the peak method.

Document code: A **Article ID:** 1673-1905(2023)03-0170-4

DOI https://doi.org/10.1007/s11801-023-2149-3

The high-precision detection of the interferogram's zero optical path difference (ZOPD) position is critical. On the one hand, the accuracy of the ZOPD position affects the accuracy of spectral recovery and infrared gas analysis[1]. On the other hand, since the infrared gas analyzer starts sampling from the ZOPD position (i.e., the scanning start position), the ZOPD position detection algorithm can be applied to the detection of the scanning start position. At present, the scanning starting position detection methods include the position sensitive detector (PSD) method, the mechanical part positioning method, etc. Compared with these methods, the ZOPD position detection method of infrared interference signals does not require additional components, optimizes the structure of the interference system, and improves its stability. This paper will study the ZOPD position detection algorithm based on wavelet transform.

Processing algorithms of interferograms' ZOPD position detection can be classified into two categories. One is to determine the maximum point of the light intensity amplitude as the ZOPD position by analyzing the interference signal's light intensity distribution[2-4]. For example, GUILLAIN et al[5] used the center of gravity method to determine the maximum position of the interference fringe's modulation and then determine the ZOPD position. SHI et al[6,7] extracted the signal envelope following frequency low-pass filtering and time-domain mean filtering, and determined the maximum position of the interference signal via the envelope maximum, that is, to determine the ZOPD position. The other method is to determine the ZOPD position by analyzing the phase information contained in the interference signal[8-10]. For instance, FENG et al[11] determined the ZOPD position using the linear relationship between the phase error caused by the interference fringe's translation and the wavenumber, then corrected the offset of the ZOPD position using the residual phase method for linear regression analysis. SHAO et al[12] employed the maximum correlation method and the calibration spectral imaginary part minimum method to determine the ZOPD position of the interference signal. WEI et al[13,14] not only successfully acquired the ZOPD position of a pulse train interferometer using phase information and a frequency pair model, but also realized that the second harmonic interference fringe phase[15] was used as a position marker for the ZOPD position detection in a nonlinear pulse train interferometer.

To further improve the accuracy and reliability of the ZOPD position detection, a ZOPD position detection method based on wavelet transform[16-18] is proposed, which simultaneously combines phase and amplitude information. In contrast to amplitude information, phase information is less susceptible to amplitude noise, which can make up for the ZOPD position error determined by the amplitude information[19,20].

A wavelet function is a collection of functions that are

* This work has been supported by the National Natural Science Foundation of China (No.42075135), and the Key Research and Development Projects in Anhui Province (No.202104a05020026).

** E-mail: xhan@aiofm.ac.cn

created by stretching and translating the wavelet-generating function. Assuming that the scale factor is a and the translation factor is b, the wavelet function can be written as follows

$$\varphi_2(x,a,b)=\frac{1}{\sqrt{a}}\varphi_1\left(\frac{x-b}{a}\right), \tag{1}$$

where φ_1 is the wavelet generating function, φ_2 is the wavelet function, and x is the independent variable.

For any square-integrable function, the one-dimensional continuous wavelet transform has the following expression form:

$$W(a,b)=\int_{-\infty}^{+\infty}f(x)\varphi_2^*(x,a,b)\mathrm{d}x, \tag{2}$$

where $*$ represents the conjugate operator, and $\varphi_2(x, a, b)$ is the wavelet basis function of the wavelet transform.

Changes in the scale factor a reply to changes in the signal f frequency, whereas changes in the translation factor b correspond to changes in the signal f displacement. The size of the correlation between $\varphi_2(a, b)$ and signal f at various frequencies and displacements can be determined by changing the scale factor a and the translation factor b continuously. The inner product connection $W(a, b)$ between the function and the wavelet sequence describes the degree of similarity between the function and the wavelet sequence function.

Given that the interference signal has Gaussian distribution features and the Morlet wavelet is modulated by a Gaussian function[8], the Morlet wavelet can be selected as the wavelet generating function of the wavelet transform with the complex expression in the form of

$$\psi(z)=\exp(-\frac{z^2}{L_w})\cdot\exp\left(\mathrm{j}2\pi w_0 z\right). \tag{3}$$

As the sampled signal is discrete, the discrete wavelet transform is required for the wavelet analysis of the interferometric signal. The following series is defined:

$$\psi(n)=\exp\left[-\left(n\Delta z/L_w\right)^2\right]\exp\left(\mathrm{j}\left(2\pi v_0 n\Delta z\right)\right), \tag{4}$$

where L_w is the infrared light source coherence length, Δz is the interferometric signal sampling interval, and v_0 is the central wavenumber of the interferometric signal.

The Morlet wavelet family can be expressed as

$$\varphi(n,a,b)=a^{-\frac{1}{2}}\psi(\frac{n-b}{a}). \tag{5}$$

For the interferometric light signal, the wavelet transform is calculated as

$$WT(a,b)=\sum_{n=1}^{N}X(n)\varphi^*(n,a,b). \tag{6}$$

For an arbitrary position, the wavelet coefficients are calculated as

$$|WT(a,b)|=\sqrt{WT_r^2(a,b)+WT_i^2(a,b)}, \tag{7}$$

where $WT_r(a, b)$ is the real part of the Morlet wavelet transform, $WT_i(a, b)$ is the imaginary part of the Morlet wavelet transform, and $|WT(a, b)|$ is the wavelet coefficient.

After wavelet processing, the phase information for any point is

$$\varphi(a,b)=\arctan\left(WT_i(a,b)/WT_r(a,b)\right). \tag{8}$$

The wavelet analysis signal area gradually varies while a and b are changing. $WT(a, b)$ will attain a maximum when it reaches a region where the wavelet function's oscillation frequency is equal to the signal frequency. When analyzing the interference signal, the center frequency of the Morlet mother wavelet is tuned to coincide with the interference signal's center frequency. As a result, the value of the parameter a can be set to 1. In this situation, the only parameter that needs to be changed is b (1, 2, 3,..., N), which can make the Morlet subwavelet slide over the signal and extract the wavelet coefficients. That is, we may obtain the signal's wavelet envelope by way of the Morlet wavelet transform. The maximum modulation position of the wavelet envelope is the position of zero-order fringe, and its phase value is φ.

According to the amplitude and phase information of the interference signal obtained by wavelet transform, the ZOPD position after deviation compensation can be calculated as follows

$$h=\Delta z\times p-\Delta z\times N\times\varphi/2\pi, \tag{9}$$

where p is the maximum modulation position of the interference signal, N is the number of sampling points in the phase interval of $(-\pi, \pi]$, where the zero-order fringe is located, and the phase value of the maximum modulation position is φ.

The schematic diagram of the error between the maximum sampling intensity position and the ZOPD position is shown in Fig.1.

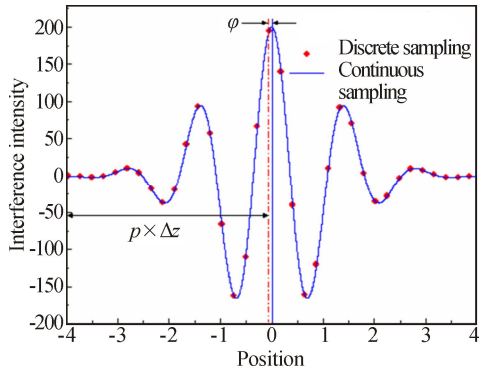

Fig.1 Schematic of the sampling deviation at the maximum intensity position

The algorithm flow chart for determining the ZOPD position based on the wavelet transform is shown in Fig.2.

The experimental data were collected using a self-developed Fourier transform infrared spectrometer. The portable Fourier transform infrared spectrometer's working principle is depicted in Fig.2. The instrument is designed with a Michelson interferometer as its core, which can quantitatively analyze atmospheric pollution gases. The interferometer's primary components are a beam splitter, a moving mirror, and a fixed mirror. As shown in Fig.3, the infrared light from the infrared light

source passes through the beam splitter. Ideally, 50% of the light is reflected back to the beam splitter after being reflected to the moving mirror, and the other 50% of the light passes through the beam splitter to the fixed mirror and then reflected back to the beam splitter, which results in an optical path difference and interference. When the optical path difference is zero, the phases of the two beams reflected by the beam splitter from the fixed mirror and the moving mirror are the same, and the light intensity after superposition is the sum of the intensities of the two beams. When the moving mirror moves a quarter of the wavelength, the optical path difference is a half wavelength. At this time, the phases of the two beams are opposite, and the light intensity is zero after superposition. When the moving mirror moves another quarter of the wavelength, the optical path difference is one wavelength, the phase difference between the two beams is one wavelength, and the phase is the same. The interference signal is formed when the moving mirror moves at the same speed over time. The signal intensity detected by the detector changes in cosine to form the interference signal.

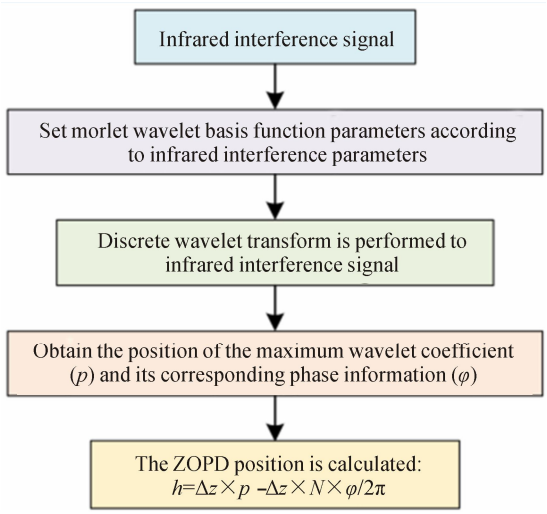

Fig.2 Algorithm flow chart based on the wavelet transform

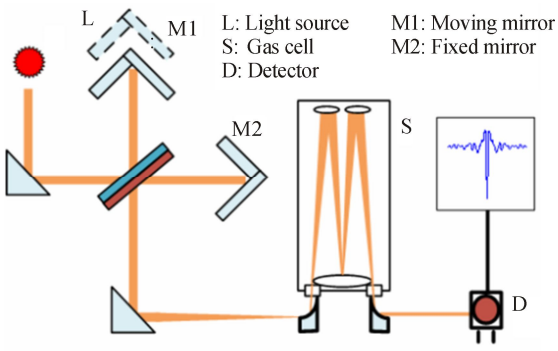

Fig.3 Working principle of the portable Fourier transform infrared gas analyzer

Twelve experiments were carried out in this study, with each experiment generating eight groups of experimental data. Taking into account that the detector hasn't been completely cooled after the equipment is turned on, the first few experiments of data with significant noise signal are discarded, and the middle 80 consecutive groups of experimental data are collected. When there are eight consecutive groups of data, they are averaged once, and 10 groups of interference data are made out of that.

The ZOPD position for the interference signal collected by the infrared gas analyzer is determined by the wavelet transform method and the peak value method, respectively, as shown in Fig.4.

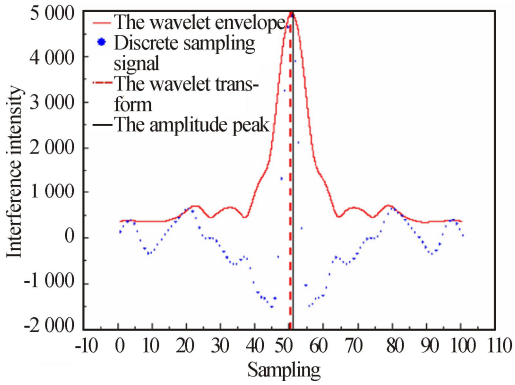

Fig.4 ZOPD position for the wavelet transform method and the amplitude peak method

The ZOPD detection error of the amplitude peak method is mainly caused by sampling error. Theoretically, the smaller the sampling interval is, the smaller the error of the amplitude peak method is. Therefore, under the same conditions, 1/10 of the original sampling interval (i.e., the sampling interval is $\lambda/20$, where λ is the wavelength of the Helium-Neon laser) is used for interference signal sampling, and the ZOPD position of the interference signal is obtained as a relatively accurate position. For the interference signal data under the original sampling interval (i.e., the sampling interval is $\lambda/2$), the ZOPD position is obtained by using the amplitude peak method and the wavelet transform method, respectively, as shown in Tab.1. Compared with the relatively accurate position, the error of the amplitude peak method is 284.76 nm and the error of the wavelet transform method is 19.617 nm. The relative error is reduced by 93.11%.

This paper proposes a high-precision detection method of the ZOPD position based on the wavelet transform. The process is essentially divided into two steps. Firstly, the amplitude and phase information of the maximum modulation position of the infrared interference signal are extracted by wavelet transform, and then the position of ZOPD is calculated by combining the phase and amplitude information. The phase information is not easily affected by the amplitude noise, and the ZOPD position error determined by the amplitude information can be compensated through phase information, which can improve the accuracy of the ZOPD position detection. The

Tab.1 Consecutive measurement results

Experiment	Relatively accurate position	Amplitude peak	Wavelet transform
1	15 851.64	16 136.4	15 838.984
2	15 851.64	16 136.4	15 905.428
3	15 851.64	16 136.4	15 842.148
4	15 851.64	16 136.4	15 895.936
5	15 851.64	16 136.4	15 823.164
6	15 851.64	16 136.4	15 905.428
7	15 851.64	16 136.4	15 826.328
8	15 851.64	16 136.4	15 842.148
9	15 851.64	16 136.4	15 924.412
10	15 851.64	16 136.4	15 908.592
Average	15 851.64	16 136.4	15 871.257
Relative error	-	284.76	19.617

experimental results show that compared with the amplitude peak method, the ZOPD position error determined by the wavelet transform method is 19.617 nm, and the relative error is reduced by 93.11%.

Statements and Declarations

The authors declare that there are no conflicts of interest related to this article.

References

[1] WEI D, AKETAGAWA M. Securing noise-adaptive selection of interference signal by nonlinear detection[J]. Optics express, 2018, 26(15)：19225-19234.

[2] HUANG Y L, GAO J, ZHANG L Y, et al. Fast template matching method in white-light scanning interferometry for 3D micro-profile measurement[J]. Applied optics, 2020, 59(4)：1082-1091.

[3] HU C, LIU X J, YANG W J, et al. Improved zero-order fringe positioning algorithms in white light interference based atomic force microscopy[J]. Optics & lasers in engineering, 2018, 100：71-76.

[4] YANG W J, LIU X J, LU W L, et al. A novel white light interference based AFM head[J]. Journal of lightwave technology, 2017, 35(16)：3604-3610.

[5] GUISLAIN B G, HARVEY R, TOKARYK D W, et al. An alternative approach to interferogram collection and processing for a vintage Bomem DA3 Fourier transform spectrometer[J]. Journal of molecular spectroscopy, 2019, 364：111181-111187.

[6] SHI Z H, YANG B X, HU X B, et al. Lens surface distance measurement with large range and high precision based on low coherence interferometry[J]. Acta optica sinica, 2016, 36(6)：06120011-06120018.

[7] LEI Z L, LIU X J, ZHAO L, et al. A rapid measurement method for structured surface in white light interferometry[J]. Journal of microscopy, 2019, 276(3)：118-127.

[8] WANG C L, LI Y S, LIU X B, et al. Detection and correction of linear phase error for Fourier transform spectrometer using phase correction method[J]. Advanced materials research, 2011, 225-226：293-296.

[9] ZHOU Y F, CAI H Z, ZHONG L Y, et al. Eliminating the influence of source spectrum of white light scanning interferometry through time-delay estimation algorithm[J]. Optics communications, 2017, 391：1-8.

[10] XIN L, LIU X, YANG Z M, et al. Three-dimensional reconstruction of super-resolved white-light interferograms based on deep learning[J]. Optics and lasers in engineering, 2021, 145(12)：106663.

[11] FENG X, GUO Q, HAN C P, et al. Correction method of zero path difference position[J]. Journal of infrared and millimeter wave, 2017, 36(006)：795-798.

[12] SHAO C Y, GU M J, QI C L, et al. Detection of zero path difference position for FY-3D hyper-spectral infrared atmospheric sounder[J]. Optics and precision engineering, 2020, 28(12)：2573-2580.

[13] WEI D, NAGATA Y, AKETAGAWA M. Phase information-assisted method to obtain the position of zero optical path difference for a pulse-train interferometer[J]. Optical engineering, 2018, 57(11)：114106.

[14] WEI D, YANG P, XIAO M Z. Frequency pair model for selection of signal spectral components to determine the position of zero optical-path difference in a pulse-train interferometer[J]. Optics communications, 2018, 434：124-127.

[15] WEI D, XIAO M Z. Using the phase of second-harmonic interference fringes as a position marker for detecting the zero optical path difference in a nonlinear pulse-train interferometer[J]. Optical engineering, 2019, 58(3)：034106.1-034106.4.

[16] SERIZAWA T, SUZUKI T, CHOI S, et al. 3-D surface profile measurement using spectral interferometry based on continuous wavelet transform[J]. Optics communications, 2017, 396：216-220.

[17] WANG Z Y, LIU Z G, DENG Z W, et al. Phase extraction of non-stationary interference signal in frequency scanning interferometry using complex shifted Morlet wavelets[J]. Optics communications, 2018, 420：26-33.

[18] SHABANI Z, SABOURI S G, KHORSAND A. Combination of discrete wavelet transform and ANFIS for post processing of spectroscopic signals[J]. Optical & quantum electronics, 2018, 50(10)：359.

[19] DENG Q Y, HUANG Q Q, HOU J, et al. Analysis and restriction about accumulated phase error in spacial frequency-domain algorithm for white-light interferomety[J]. Laser & optoelectronics progress, 2021, 58(7)：0718001.1-0718001. 11.

[20] ZHOU Y F, ZHONG L Y, CAI H Z, et al. White light scanning interferometry based on generalized cross-correlation time delay estimation[J]. IEEE photonics journal, 2017, 9(5)：6900511.